Engineering Chemistry
ISSN: 2813-6535, Vol. 13, pp 105-118
doi:10.4028/p-SnxM3n

Submitted: 2025-09-21
Accepted: 2025-10-17
Online: 2026-02-18

A Comparison Study between Steady-State and Dynamic Operation Models on The HTPS Performance

Zahraa Yahya Al-Moosawi[1,a*], Adnan A. Ateeq[2,b], Maher T. Al Shamkhani[3,c]

[1*]Thermal Mechanic Engineering Department, Basrah Engineering Technical College, Southern Technical University, Iraq

[2]Chemical and Petrochemical Engineering Department, Basrah Engineering Technical College, Southern Technical University, Iraq

[3]Fuel and Energy Engineering Department, Basrah Engineering Technical College, Southern Technical University, Iraq

[a*] zahraa.y.faker@fgs.stu.edu.iq, [b]dn.betc@stu.edu.iq, [c]maher@stu.edu.iq

Keywords: HTPS, Performance Enhancement, Aspen HYSYS V14, operation Parameters, Dynamic and Steady-State Model.

Abstract. Given the importance of enhance the performance of oil separators in production field, this research study the separation process through simulations based on a real field data, WQ-2 south of Iraq-Basra. By implementing both dynamic and steady-state approaches in Aspen HYSYS V.14, the optimization was carried out for each approach for comparison. Results from the steady-state simulation revealed limited improvement, with closely converging iterations and changes applied to only one variable at a time. In contrast, the dynamic simulation given more realistic and favorable results, as manual adjustments were applied in a real-time response to the actual field dynamics range and conditions. The result shows that the maximum OVFR=15050 m^3/h and CO=0.1999099 at T= 60 °C and P= 15 barg for static model, while the OVFR=1580.9 m^3/h, CO=0.0093 at P=14 barg, T=76 °C where the operation time 120 min for dynamic. Compared to the static approach, the dynamic approach was efficient to reach better performance when the selected parameters were optimized and that led to a substantial improvement in the separation efficiency. Therefore, the dynamic simulation could be considered a mandatory approach when the overall separator efficiency need to be enhanced.

Introduction

Oil and gas separators, particularly Horizontal Three-Phase Separator (HTPS), are considered the main equipment in oil production facilities. The separators are designed to separate the hydrocarbon compounds into their various components for both single-phase and multi-phase flow systems and delivering the output as distinct streams. However, handling single-phase fluids is technically less complex compared to the treatment of multi-phase fluids and is more economical due to the lower energy requirements during flow [1]. These separators can be classified based on configuration vertical (VS), horizontal (HS), and spherical or by their functional role in phase separation. Moreover, both vertical (VS) and horizontal (HS) separators are commonly used for three-phase flow separation. They may also be categorized by operating conditions such as operating pressure, allowing classification into high, medium, and low-pressure separators as referenced by [2, 3]. Also, the gravity has been considered one of the operational challenges that could result in the complicity of the separators [4]. In order to optimize the performance of the (HTPS), the optimization could be conducted by using two different approaches which were static and dynamic. Both approaches depended on gravity, retention time, internal design, and operational parameters [5, 6, 2]. To achieve effective phase separation, there are several parameters effecting the HTPS performance such as temperature, pressure and retention time [7]. The effect of retention time has been demonstrated indicated that increasing the fluid hold-up inside the vessel enhances phase stratification but necessitates a larger separator volume [8]. The latest confirmed Arnold theory which that significantly improves phase stratification and separation efficiency [9]. The second parameter is the temperature which has high impact on separation as those thermal variations influence separation efficiency and production rate [10, 11]. However higher temperatures reduce fluid viscosity, thereby enhancing OR purity [12]. Moreover, operating pressure significantly influences separation efficiency. Higher pressure (HP) tends to stabilize the phases and maximize OR [13, 14]. Also HP reduces the density differences between phases, which may impair droplet coalescence and disturb effective settling [12, 15]. Therefore, pressure must be optimized carefully to balance phase stability and separation performance. Many studies explore the parameters problem including common issues such as emulsions, foaming, and the phenomenon of "carryover"(CO) [16, 17]. CO in HTPS due to reservoir changes, causing liquid droplets to enter gas or oil streams and reducing product quality [18, 19]. Several studies have investigated the effect of operating parameters using computational tools to improve the separation processes, such as using Aspen HYSYS (AH) to optimize these parameters [13, 20, 21]. AH is commonly used as the most effective and realistic simulation tool with its capabilities supported by studies as [23, 24, 26]. Other software could be employed such as CHIMEDI and Unisim to analyze parameter impacts on the separator performance [12, 27]. In addition, CFD was used to investigate the internal design enhancements and the parameters effects [28-30]. Furthermore, Response Surface Methodology (RSM) with ANSYS Fluent were employed to assess separator performance sensitivity to baffle location, flow regime, and demister arrangement [27]. The latest study showed that increasing oil viscosity and density could elevate drag forces, promoting droplet entrainment [29, 31]. Additionally, the trade-offs between pressure drop and droplet coalescence in coalesce-baffle systems that reason of escaping masses in phases [32]. Also, Another method was used the Document Control System (DCS) to monitor the operating parameters and stably control of (central process facility) CPF process to get safe operation and stable for long-term [22]. Based on the review, the studies confirmed that the combined importance for both mechanical design and the operational parameter to reduce problems and enhance phase purity could be reached by understanding their interactions. Accordingly, unlike previous optimization studies that primarily focused on steady-state simulations or CFD-based design improvements, this study focuses on enhancing the performance of HTPS in the WQ-2 field using AH V.14 by identifying and selecting the optimum parameters. The study employed both self-optimization (using the software's built-in utilities) and manual-optimization (by directly altering feed conditions) to increase oil production and reduce liquid in gas phase. Additionally, the study was helpful to understand the impact of each parameter on oil production in multi cases and finally comparative results between both modes (static and dynamic). This work investigated by varying operating parameters within their design limits to better represent actual field conditions, to identify configurations for oil enhancement and phase purity. A comprehensive theoretical study was first conducted to evaluate the influence of three variables (temperature (T), pressure (P), and retention time (t_e)) to identify the most significant factor affecting on separation efficiency. The theoretical analysis preceded field implementation to ensure clear and reliable results. The proposed will be recommend after the validated with the real field result followed by necessary suggestions and approvals, ensuring that all potential hazards and operability issues were properly addressed before practical application in the field. The results, showed that improvements in the static model were limited and relatively uniform. Such as, manual optimization produced OVFR=1580.9 m^3/h, CO = 0.0093 at P=14 barg, T=76 °C and time 120 m, while self-optimization maximum OVFR=15050 m^3/h and CO= 0.199 at T= 60 °C and P= 15 barg while the minimize CO= 0.007984 with OVFR= 12726 m^3/h was observed at T=80 °C and P= 11.88 barg. The static mode confirmed the direct effect of pressure and temperature on production, while the dynamic model showed that increasing time significantly increased oil output and reduced liquid in gas phase, with oil rising from 1780.6 m^3/h to 1783 m^3/h from 2 to 3 h. In conclusion this research shows that manual optimization can yield robust results and provide a solid basis for further improvements.

Objective

The study novelty is to evaluate the differences between steady-state and dynamic simulation models for WQ-2 HTPS by mimic the real field and optimization the performance.

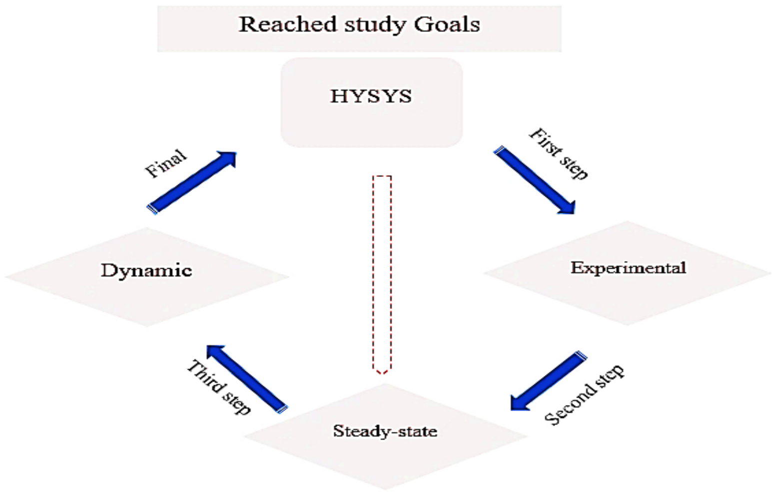

Fig. 1 The objective aim process

Methodology

AH software was used to simulate both the steady-state and dynamic operation models of WQ-2 HTPS, as Fig. 3 model flow sheet. The aimed to evaluate the performance of the HTPS and enhance production efficient under current and future operating conditions. Real field data were utilized to calibrate the models, which has production per day and per hour as Table 1 and Fig.2. The optimization process focused on modify essential operating parameters, such as P, T, and t_e. Further to assess their direct impact on oil volume flow rate and liquid in gas phase. Finally, comparative analysis was conducted between the steady-state and dynamic models to highlight performance differences and validate operational improvements.

Table 1. Oil production per day and per hour with separation phases – real field data

Total oil Production m^3/day	oil m^3/day	Water m^3/day	Gas m^3/day
2893436.17	108866.38	12061.67	2672508.12
Total oil Production m^3/h	oil m^3/h	Water m^3/h	Gas m^3/h
1068.49	968.49	120.66	40273.09

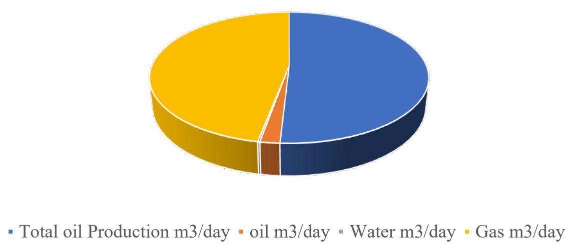

Fig.2 Oil production per day

Simulation process

This study used AH to mimic the performance of HTPS. First a model consisting of eight linked separators was developed based on the configuration of the WQ-2 field (Aspen Technology Documentation Team 2005). Second, both steady-state and dynamic models were constructed to compare simulation outputs with actual field data and optimize operational performance [23,33]. Related to thermodynamic packages were applied by AH environment to achieve energy balance and phase equilibrium calculations[34,35]. This study was for mimic that models and compare it with real flied then optimized it to minimize liquid in gas phase that to improve both oil outcome with purity. However, the simulation results can never exactly replicate real field outcomes due to the inherent complexities and dynamic nature of actual production environments.

Table 2. Field Design Data for Total Feeds

Conditions	
Temperature [◦C]	60-120
Pressure [Barg]	8-15
Molar Flow [Kgmole/Day]	12,297,103.7
Mass Flow [Kg/Day]	2,459,420,744.5
Std Ideal Liq Vol Flow [M^3/Day]	2893436.17

Simulation package

Related to the selection of high-pressure (HTPS) and the need to improve oil separation based on density, the Peng–Robinson package(PR) was adopted due to its higher accuracy in representing both liquid and gas phases under a wide range of pressures and temperatures compared with the Soave–Redlich–Kwong (SRK) equation [12,36]. Its main function to calculate the thermodynamic properties of fluids in both the liquid and vapor phases, thereby estimating the behavior of mixtures inside HTPS. Moreover, it is widely used in oil and gas applications, especially under medium to high pressures, and is preferred over other models equations, due its superior handling of temperature, pressure, and fluid composition [37]. Peng–Robinson Equation of State (EOS) was used to estimate K-values, vapor pressure, and liquid density, based on critical properties and acentric factors [38, 39]. It provides the simulation program or manual calculations with the values that determine how the components are distributed between the phases. Using the EOS (Eq. 1), the thermodynamic properties of both phases were estimated [40]. This package includes several objective variables, such as the repulsion parameter (Eq. 2, Eq. 3), the attraction parameter a (Eqs. 4–6) [24], and the critical properties (critical pressure, critical temperature, and critical volume) (Eqs. 2-7) [12]. It also evaluates the compressibility factor of the phases (Eq. 10) [41], the fugacity of each component in every phase (Eq. 12) [38], and the equilibrium ratio (K-value) (Eq. 15) [19, 38] see Equations below:

$$P = \frac{RT}{V-b} + \frac{a}{(V^2 + Vb) + b(V-b)} \quad (1)$$

$$bi = o.o77796 \times (\frac{RTci}{Pci}) \quad (2)$$

$$b = \Sigma\, xi \times bi \quad (3)$$

$$ai = \alpha i \times aci \quad (4)$$

$$aci = o.457235 \times (R^2 \times \frac{Tci^2}{Pci}) \quad (5)$$

$$\alpha i = [1 + mi \times (1 - Tri^{1/2})]^2 \quad (6)$$

$$Tri = \frac{Ti}{Tci} \quad (7)$$

$$mi = 0.37464 + (1.54226\omega i) - 0.26992\omega i^2 \quad (8)$$

$$\mathrm{a} = \Sigma\,\Sigma\, \mathrm{x}i\ \mathrm{xj}\left((\mathrm{a}i\ \mathrm{aj})\right)^{1/2} (1 - \mathrm{kij}) \quad (9)$$

Where a,b: Substance-specific Peng–Robinson parameters (related to attraction/repulsion between molecules), mi : Coefficient used in temperature correction of EoS, ω i : Acentric factor (unitless).

$$Z^3 - Z^2 + (A - B - B^2)Z - AB = 0 \quad (10)$$

$$\mathrm{Z}^3 - \mathrm{Z}^2 + \mathrm{BZ}^2 + (\mathrm{AZ} - 2\mathrm{BZ} - 3\mathrm{B}^2\mathrm{Z}) + \mathrm{AB} - \mathrm{B}^2 - \mathrm{B}^3 = 0 \quad (11)$$

$$\ln(\phi i) = -\ln(Z - B) + (Bi\,Z - Bi) - \left(\frac{A}{(2.82843B)) \times (Ai - Bi)}\right) \times \ln\left[\frac{(Z + 2.4142B)}{(Z - 0.4142B)}\right] \quad (12)$$

where;

$$A = \frac{aP}{(RT)^2} \qquad B = \frac{bP}{(RT)} \qquad Bi = \frac{bi}{b}$$

$$Ai = \frac{1}{a} \times [2 \times ai^{1/2} \times \Sigma\, xj \times aj^{1/2}(1 - kij)] \quad (13)$$

$$Ki = \frac{yi}{xi} = \frac{\Phi il}{\Phi iv} \quad (14)$$

Where A, A_i, B, and Bi are simulator coefficients of empirical. Additionally, Φi is the fugacity coefficient of component i, Φil is the fugacity coefficient of component i in liquid phase, Φiv is the fugacity coefficient of component i in vapor phase, Ki is the K-value of component, and yi is the mole fraction of component i in the vapor phase.

Optimization steps:

The optimization was in two ways as outlined below. The procedure involved adjusting operational parameters, such as T, P, and t_e to identify the optimal conditions[42, 43]. The constraints of operating limits and safety margins should be limited within design range as table 2.

Self-optimization:

That method is a mimic-driven type that employed a specific mathematical rules and structured algorithms to identify the optimal operational configuration. This method is commonly applied within steady-state models due to its inherent limitations in capturing dynamic system behavior. It is particularly effective when the objective is to evaluate and enhance separator performance under a fixed set of conditions[24, 27]. The select Consist by objective Function: It is a function of a mathematical expression that evaluates and optimizes outcome performance by objective temperature, pressure and vessel level and maximizing OVFR production with minimizing liquid in gas phase by inputs variables. Subject to: ($P_{min} \leq P \leq P_{max}$) ($T_{min} \leq T \leq T_{max}$).

Table 3. Optimization objective Description

Variable	Type	Description
Temperature (T)	Independent	The operating temperature (°C) of the feed Separator
Pressure (P)	Independent	The operating pressure (barg) of the feed Separator
oil Flowrate	Dependent	oil volume flow rate in the liquid phase
Carryover	Dependent	Amount of liquid (kg/h or vol%) in the gas phase

Manual optimization:

This optimization by changing parameters manually on feed to get the optimum input to reach the optimized goal, in dynamic model with time adjusted as Fig. 5.

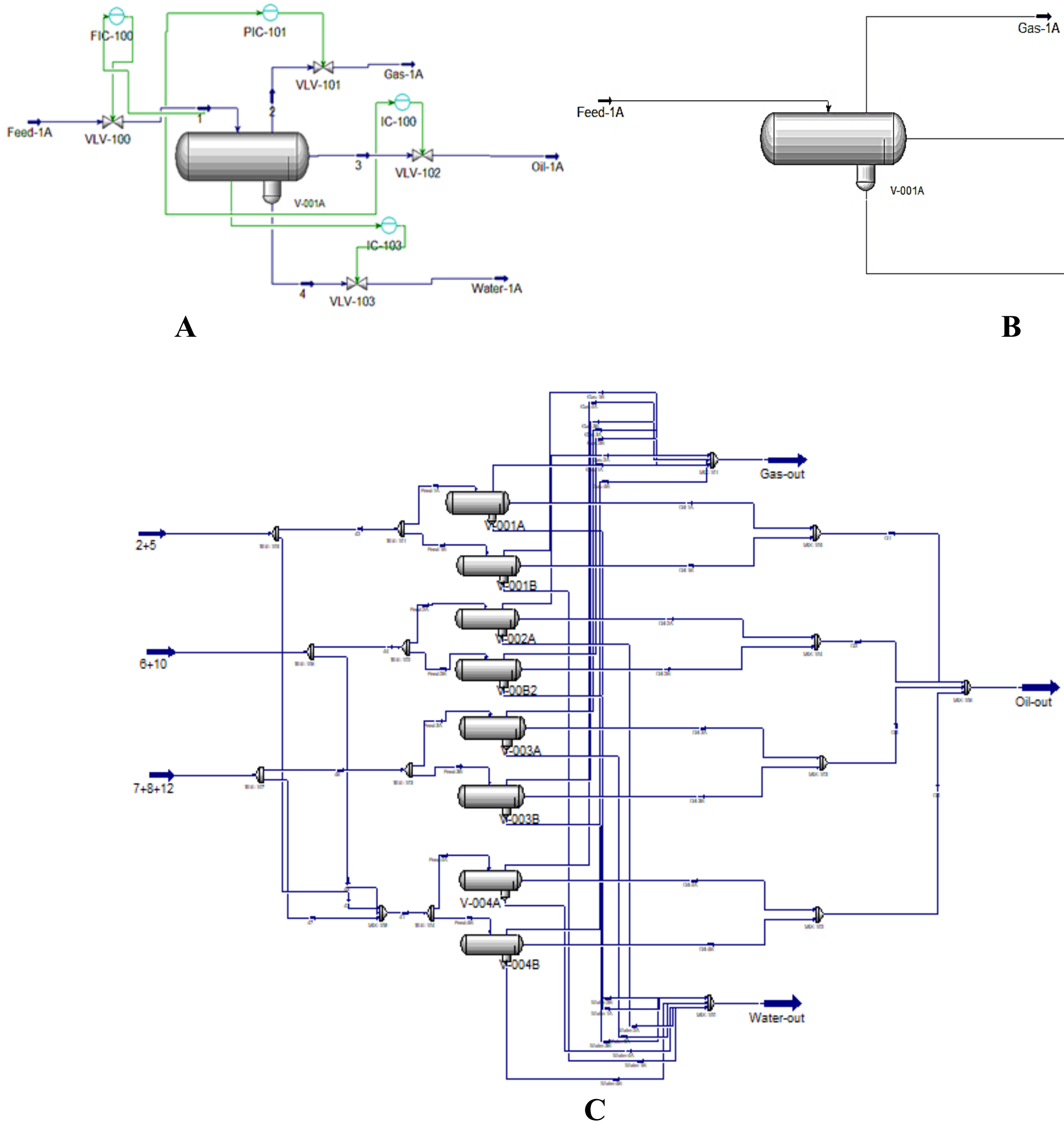

Fig. 3 HYSYS models (A: Dynamic, C B: Static C: 8 Separator)

Results and Discussion

Simulation and optimization:

The simulation results were valid with the real field data for both models, with acceptable error [45] as Table 4 and Fig. 6. For a single separator, the static model yielded OVFR = 996.00 m³/h, WVFR = 102.50 m³/h, GVFR = 40,205.81 m³/h, and CO = 0.089, while the dynamic model gave OVFR = 1002 m³/h, WVFR = 99.10 m³/h, GVFR = 40,260 m³/h, and CO = 0.088. In the dynamic model, due to time dependence and initial instability of the liquid phase, the separation gradually stabilized over time. For instance, OVFR started at 200 m³/h at 35 min and reached 1002 m³/h at 120 mint as adjusted see Fig. 7.The real field measurements were OVFR = 968.49 m³/h, WVFR = 120.66 m³/h, GVFR = 40,273.09 m³/h, and CO = 0.2 at P = 10 barg and T = 66°C. The dynamic model effectively mimicked this behavior, showing performance variations over time, starting with unstable operation and gradually achieving optimal separation as observed in the field. In conclusion, the dynamic simulation of eight separators resulted in OVFR = 110,640.04 m³/day, slightly higher than the static model value of OVFR = 109,640.2 m³/day, This deviation was due to flow fluctuations and control valve adjustments, which represent one of the study challenges see Fig. 6 (b).

Table 4 Stander error between AH and real Data

RATE	(OVFR)-REAL	(OVFR)-STATIC	SSRE
OVFR	968.49	996	0.000806846
RATE	**(OVFR)-REAL**	**(OVFR)-DYNMIC**	**SSRE**
OVFR	968.49	1002	0.001118442

Self-Optimization: The results show limited and closely spaced iterations, as Table 5 and Fig. 4. Moreover, the optimization target was achieved through the automatic selection and gradual adjustment of multiple parameters to calculate the variables select of the current separator. Result show the maximum OVFR=15050 m^3/h (objective Function 1) and CO=0.1999099 (objective Function 2) at T= 60 °C and p= 15 barg while the minimize CO=0.007984 with OVFR= 12726 m^3/h was observed at T=80 °C and P= 11.88 barg as Table 4 and see Fig. 9 parameters effect on OVFR and CO. As a result, the goal of simultaneously increasing OVFR while decreasing CO with a balanced set of optimal parameters was not achieved.

Table 5. Self-optimization result by AH

Iteration	Cum. Func. Eval.	Objective Function 1	T [c°]	P [bar.gl]	Objective Function 2
1	3	12726	80	11.8835	0.007984
2	3	11828	80	10.3835	0.009992
3	7	12557	74	10.4487	0.099923
4	11	13276	68	10.6294	0.197834
5	15	14015	62	11.0093	0.189800
6	19	14446	60	11.5940	0.1980101
7	23	15050	60	13.0940	0.1999099
8	27	15579	60	14.5940	0.202390
9	31	15712	60	15	0.29890

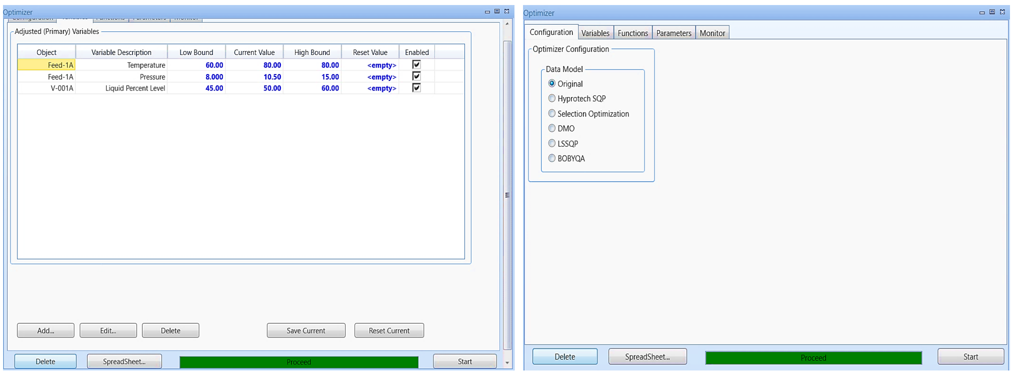

Fig. 4. Objective function with variables by AH of steady state (static model)

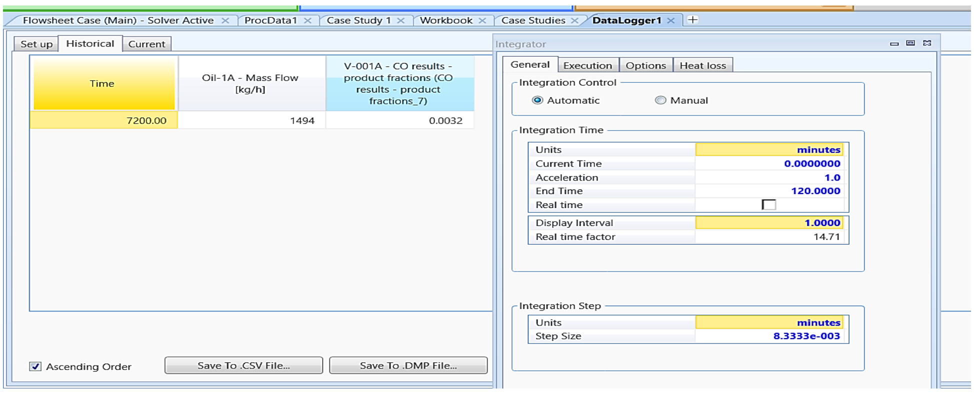

Fig. 5. Time adjusted by AH for dynamic model (screen shot)

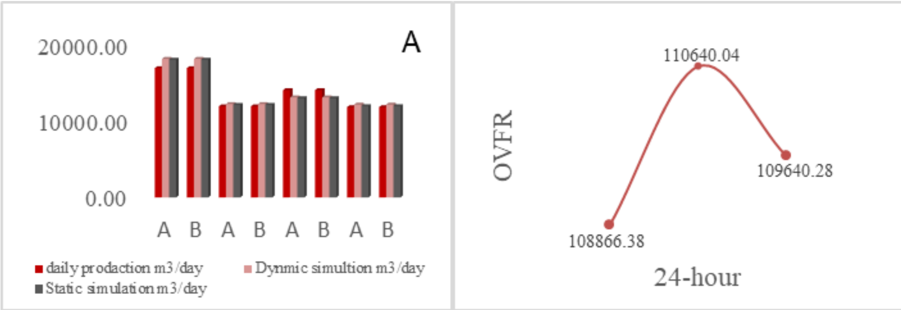

Fig.6. The comparison for Oil production (A) Oil production m^3/day real and simulation single 8 HTPS, (B) dynamic vs. static model deviation isfrom real field oil production

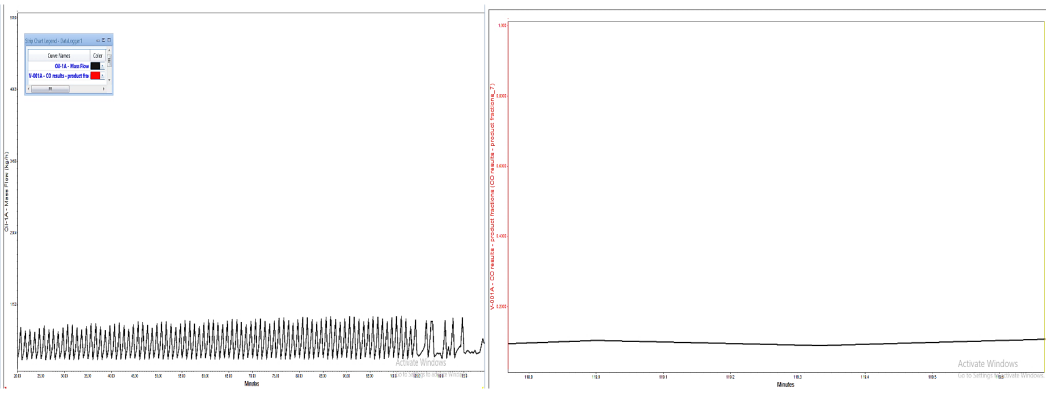

Fig. 7. The dynamic model demonstrates liquid instability until a steady state is achieved, a result by AH.

Dynamic optimization: While changing feed parameters manually, the results showed that each variable reached its target when the balance parameters were selected. For example, increasing the P required increasing the T by 2 °C, either through trial and error or by calculating the optimum P using estimated values and fixing the P with the equations described above, which represented the third challenge of the study. In dynamic model, the enhanced results showed OVFR = 1780.6 m³/h and CO = 0.0087 at P = 11 barg, T = 73 °C, and 120 min, while increasing the parameters to P = 13.5 barg, T = 76 °C, and 120 min resulted in OVFR = 1580.9 m³/h and CO = 0.0093 see Fig. 10 for the enhancement of OVFR under manually changed parameters in dynamic model. Although this stage provided a more accurate representation of real operational conditions, it posed challenges related to input precision and simulation time requirements see Fig. 4. This value couldn`t be directly compared with the static model due to differences in calculation methods and input parameters, as well as the inclusion of time effects and parameter equilibration in the dynamic model.

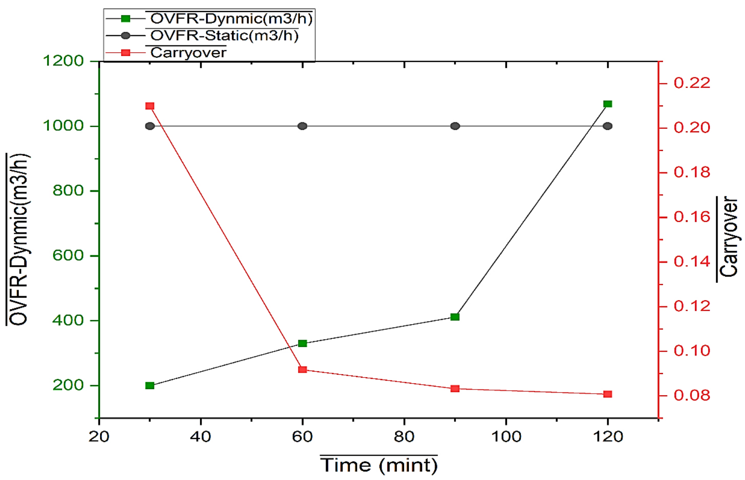

Fig. 8. The different between both model (static &dynamic) on OVFR with time and CO

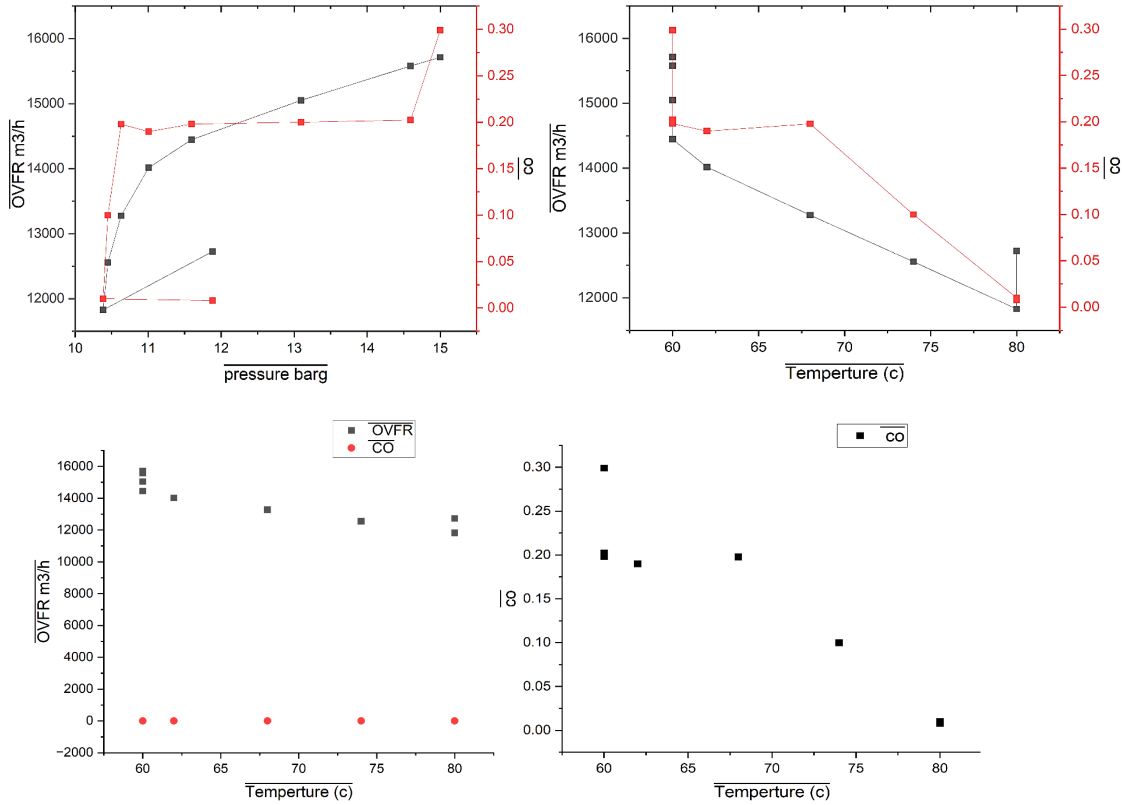

Fig. 9 Result of self-optimization (static model) for OVFR and CO by 2 parameters(T,P)

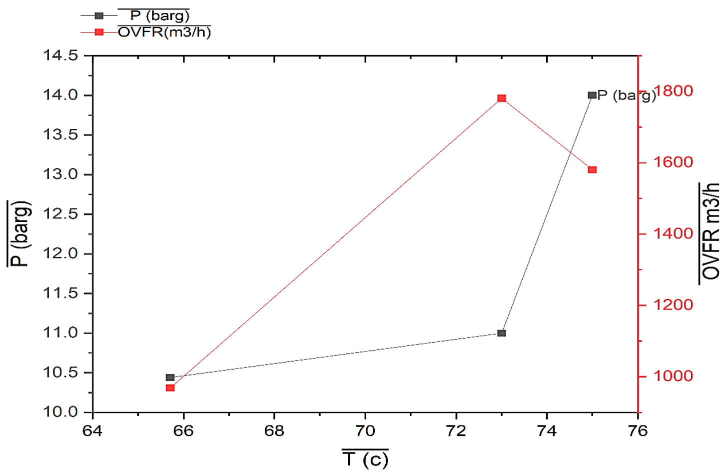

Fig. 10. Result of manual-optimization (dynamic model) for OVFR with parameters (T, P)

Parameters effect:

Pressure effect: At Increased pressure that suppresses gas liberation but improve Oil production. However, excessively high pressure (HP) causes CO due to liquid entrainment in the gas phase as Fig.11 [44].As that supported by Al-Mahna (2018) P influences phase behavior and droplet coalescence also the HP causes a reduction in the boiling point. Nath (2022) the importance of selecting optimal P important based on feed properties such as Gas-oil Ratio and API gravity to minimize CO. Also its effected on the stages while optimized OR but not redaction CO[13, 14].

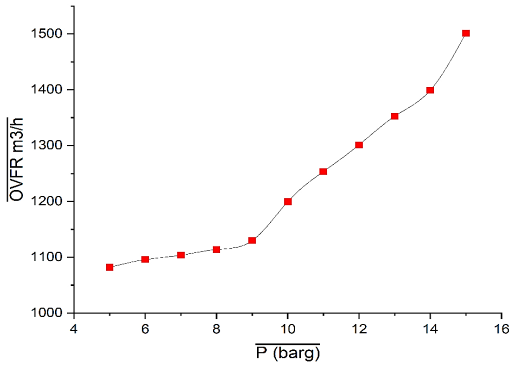

Fig. 11. Pressure Effect demonstrates by Cases Study on OVFR

Temperature Effect: The study show increasing the T of feed significantly enhance separation. While effect on the oil properties with promote vaporization inside the separator, leads to free the gases with reached liquid purity related raised oil density as Fig. 12 explanation OVFR max and min value with P [11]. Also its affecting separation efficiency alongside droplet size and t_e[11, 22]. that reduce CO as the study Shaban (1995) found that higher temperatures reduce CO and supported by Bothamley (2017) noted that increased T lowers oil viscosity and increases the settling velocity of water droplets and also Al-Mahna (2018) noted raising the inlet T can causes change in the outlet vapor mass flow rate that comes from the HP separator.

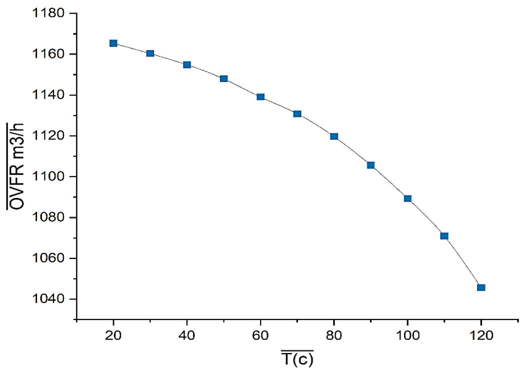

Fig. 12. Temperature Effect demonstrates by Cases Study OVFR

Retention time effect: In our study the result show at increase t_e that effect on separator process. at increased time in dynamic mode from 120 min to 150 min, with P and T constant, the separator performance improved as (P = 11 barg and T = 73 °C) OVFR Increased (from 1780.6 m^3/h to 1783 m^3/h) and CO reduced (from 0.0087 to 0.00859) but at(P = 14 barg and T = 75 °C) OVFR increase (from (1580.9 m^3/h to 1582.1m^3/h) and the CO reduced (from 0.0093 to 0.00887) as shown in Fig. 13 and 14. Higher time enhance liquid separation by allows gravitational settling of oil and water phases, reducing droplet entrainment and improving separation [9].At longer time the separator will work in obesity way caused vacuum reaction, turbulence and low separation affect which supported by Al-Mahni (2018). Additionally, Ahmeed T. et.al. 2020 and Sampaio et al. (2010) noted the relationship between t_e (and separation efficiency and the interaction between t_e, P, and T in phase separation dynamics. while Nath (2020) and Hasan et al 2024 [13] observed stressed balancing t_e with throughput, particularly in offshore separators with space constraints. Also, the separator efficiency were influenced by retention time, with increased retention time leading to improved separator efficiency see fig. 13 and fig. 14 t_e effects on OVFR.

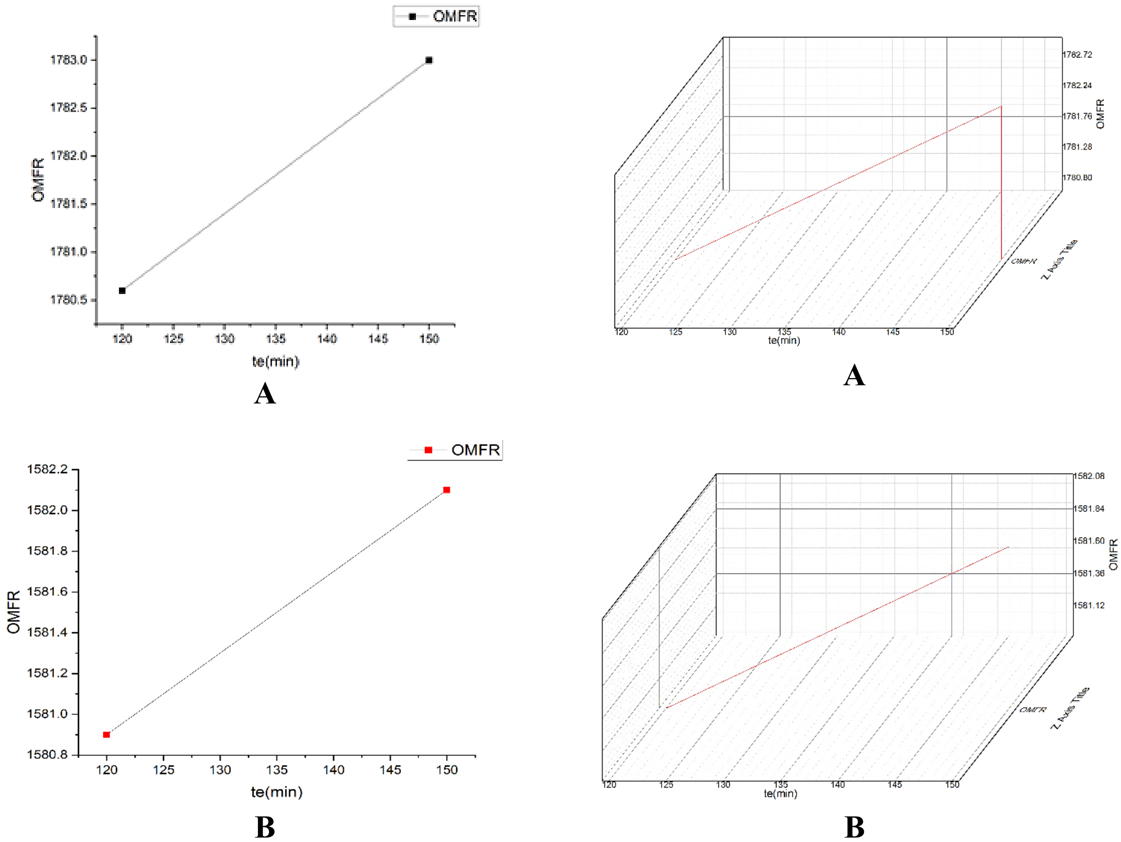

Fig.13. Comparison of Retention time effect on OVFR (A): OVFR optimization at 12o min and 15o min at feed 1 (11barg and (B): OVFR optimization at 120 min and 15o min at feed 2 (14barg and 75 c)

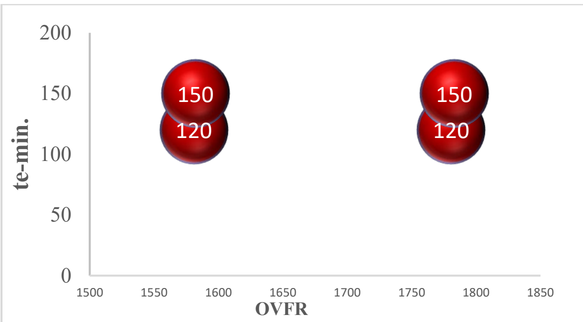

Fig.14. Retention time effect clearly for both Comparison result on OVFR

Table 6 Manual vs Automatic optimization comparative

Aspect	AH Self-optimization	AH Manually optimization
Applicability	only for steady-state conditions	Suitable for both steady-state and dynamic conditions
Responsiveness to Dynamics	Cannot model time-dependent behaviour	Captures time-based changes; reflects real field conditions
Computation Time	Longer computation time	More efficient; flexible to iterative changes
Accuracy	Lower accuracy under variable conditions	Higher accuracy due to targeted adjustments
Control Flexibility	Limited user control over optimization path	Full control over parameter tuning and response tracking
Realism	Less representative of actual operations	Closely matches field performance
outcome in this Study	Less improvement in separation performance	Achieved 100% separation efficiency after re-evaluation in AH

Conclusion

In real oil fields, changing mechanical components is not an easy task. Therefore, alternative methods that could theoretically modify production flow were studied first and then implemented practically to avoid operational risks. In this study, the performance enhancement of HTPS did not necessarily require costly mechanical modifications. Instead, significant improvements were achieved through optimization of operational parameters, (T), (P), and (t_e).Using AH, two different models steady-state and dynamic were designed and simulated. The results revealed that the dynamic model provides a more realistic representation than the steady-state model, particularly in capturing the effects of time on separation behavior and efficiency. In the steady-state model, the maximum OVFR of 15,050 m^3/h with CO = 0.199 was observed at T = 60 °C and P = 15 barg, while the minimum CO of 0.007984 with OVFR = 12,726 m^3/h was obtained at T = 80 °C and P = 11.88 barg. These variations highlight the sensitivity of CO and OVFR to parameter selection and the limited iteration space in the static model. In the dynamic model, OVFR = 1,580.9 m^3/h and CO = 0.0093 were obtained at P = 13.5 barg, T = 76 °C, and t_e = 120 min. Accordingly, it was observed that balancing the parameters provided values consistent with the optimization objectives, improving phase purity by reducing CO. A parameter effect study was also conducted under multiple cases to assess the individual effects of P, T, and t_e. The highest oil production and CO were recorded at the maximum tested P (15 barg) and the lowest T (60 °C), where lower viscosity facilitated easier separation but reduced purity in phases. This demonstrates how increasing P directly effects on OVFR. Additionally, the effect of retention time was observed, with OVFR increasing from 1,780.6 m^3/h to 1,783 m^3/h when t_e increased from 2 h to 3 h, confirming that longer retention times enhance separation. Finally, manual optimization in the dynamic model captured real-world startup behavior, showing how performance evolves over time: starting with unstable operation and gradually reaching optimal separation (steady-state). The results of this study confirmed that the dynamic simulation approach was applicable to evaluate production changes in real field conditions with enhancing the overall separation efficiency. However, the static model was helpful to understand the effect of parameters on production and phase separation in an approximate or theoretical manner, rather than replicating actual field behavior.

References

[1] Manning, F.S. and R.E. Thompson, Oilfield processing of petroleum. 1991.

[2] Arnold, K. and M. Stewart, Surface production operations, Volume 2:: Design of gas-handling systems and facilities. Vol. 2. 1999: Elsevier.

[3] Mokhatab, S., W.A. Poe, and J. Speight, Handbook of natural gas transmission and processing. Gulf Professional Publishing. 2012.

[4] Stewart, M. and K. Arnold, Gas-liquid and Liquid-liquid Separators. 2008: Gulf Professional Publishing.

[5] Ahmed, T., N. Makwashi, and M. Hameed, A review of gravity three-phase separators. Journal of Emerging Trends in Engineering and Applied Sciences, 2017. **8**(3): p. 143-153.

[6] Ahmed, T., et al., Design and capital cost optimisation of three-phase gravity separators. Heliyon, 2020. **6**(6).

[7] (DEng, D.D.H., Gas Processing. 2024.

[8] Famisa, R.B., HYSYS Modelling of a Horizontal Three-Phase Subsea Separator. 2016, NTNU.

[9] Arnold, K.E. and P.J. Koszela, Droplet-settling vs. retention-time theories for sizing Oil/Water separator. SPE Production Engineering, 1990. **5**(01): p. 59-64.

[10] de Souza Sampaio, N.A., et al., effect of pressure and temperature on the retention time of crude oil inside the three-phase separator using the response surface methodology. revista de Gestão Social e Ambiental, 2025. **19**(5): p. 1-14.

[11] Zhang, T., C. Li, and S. Sun, Effect of temperature on oil–water separations using membranes in horizontal separators. Membranes, 2022. **12**(2): p. 232.

[12] Al-Mhanna, N.M., Simulation of high pressure separator used in crude oil processing. Processes, 2018. **6**(11): p. 219.

[13] Hasan, A.F. and G.M. Farman, Optimization of Separator Size and Operating Pressure for Three-phase Separators in the West Qurna1 Oil Field. Iraqi Journal of Chemical and Petroleum Engineering, 2024. **25**(1): p. 103-110.

[14] Bahadori, A., H.B. Vuthaluru, and S. Mokhatab, Optimizing separator pressures in the multistage crude oil production unit. Asia-pacific Journal of Chemical Engineering, 2008. **3**(4): p. 380-386.

[15] Bymaster, A., et al. High pressure gas-liquid separation: an experimental study on separator performance of natural gas streams at elevated pressures. in Offshore Technology Conference. 2011. OTC.

[16] Sulaiman, F.A., et al., Mitigating Liquid Carry-Over and Foaming in a Gas Processing Plant through the Installation of Vertical Scrubbers. Petroleum Chemistry, 2024. **64**(1): p. 62-74.

[17] Shaban, H.I., A study of foaming and carry-over problems in oil and gas separators. Gas separation & purification, 1995. **9**(2): p. 81-86.

[18] Choi, M. Prediction of separator performance under changing field conditions. in SPE Annual Technical Conference and Exhibition? 1990. SPE.

[19] Sulaiman, F.A., H. Sidiq, and R. Kader, Liquid carry-over control using three-phase horizontal smart separators in Khor Mor gas-condensate processing plant. Journal of Petroleum Exploration and Production Technology, 2024. **14**(8): p. 2413-2435.

[20] Farman, G.M., Determining Optimum Oil Separator Size and Optimum Operating Pressure. Iraqi Journal of Chemical and Petroleum Engineering, 2022. **23**(2).

[21] Kotb, M., G. Abdelalim, and S. Abdall, Optimization of Oil-Gas Separation in the Production Stations at Abo-Sannan Field: Case Study. Improved Oil and Gas Recovery, 2024. **8**.

[22] Li, Z., Y. Li, and G. Wei, Optimization of Control Loops and Operating Parameters for Three-Phase Separators Used in Oilfield Central Processing Facilities. Fluid Dynamics & Materials Processing, 2023. **19**(3).

[23] GROUP-6-Separation-Operations, 7 Separation Operations.

[24] Nath, S.R., Separation Train Design and Optimaztion in Offshore Oil and Gas Production Facilities. 2022, ACS Publications.

[25] Qaroot, Y.F., Simulation of three-phase separator performance. 2013, The Petroleum Institute (United Arab Emirates).

[26] Edwin, M., S. Abdulsalam, and I. Muhammad, Process simulation and optimization of crude oil stabilization scheme using Aspen-HYSYS Software. International Journal of Recent Trends in Engineering & Research, 2017. **3**(5): p. 324-334.

[27] dos Santos Lemos, I. and L. de Sousa Santos, Analysis of multi-objective optimization applied to the simulation of a natural gas separation plant. Gas Science and Engineering, 2024. **128**: p. 205360.

[28] Jonach, T., et al., Modeling and Simulation of 3-Phase Separators in the Oil and Gas Industry with Emphasis on Water Quality. Chemical Engineering Transactions, 2022. **94**: p. 1009-1014.

[29] Carvalho, A., D. Galindo, and J. Marinho, Modeling and simulation of a horizontal three-phase separator: influence of physicochemical properties of oil. Brazilian Journal of Petroleum and Gas, 2021. **14**(4).

[30] Joshy, A., A. MA, and A. Nambiar. CFD Analysis and Optimization of Three Phase Oil Separator. in Proceedings of the International Conference on Systems, Energy and Environment. 2022.

[31] Pourahmadi Laleh, A., W.Y. Svrcek, and W. Monnery, Computational fluid dynamics-based study of an oilfield separator--Part I: a realistic simulation. Oil and Gas Facilities, 2012. **1**(06): p. 57-68.

[32] Lu, Y., J. Greene, and M. Agrawal. CFD characterization of liquid carryover in Gas/Liquid separator with droplet coalescence due to vessel internals. in SPE Annual Technical Conference and Exhibition? 2009. SPE.

[33] AspenHYSYS:ProcessSimulationSoftware.Availableonline:(accessed on 7 February 2023). 2023-2025.

[34] Gmehling, J., et al., Chemical thermodynamics for process simulation. 2019: John Wiley & Sons.

[35] Gutierrez, J.P., et al., Thermodynamic Properties for the Simulation of Crude Oil Primary Refining. 2014.

[36] Peng, D.-Y. and D.B. Robinson, A new two-constant equation of state. Industrial & Engineering Chemistry Fundamentals, 1976. **15**(1): p. 59-64.

[37] Elsharkawy, A.M. Predicting the properties of sour gases and condensates: equations of state and empirical correlations. in SPE International Oil Conference and Exhibition in Mexico. 2002. SPE.

[38] Naji, H., Conventional and rapid flash calculations for the soave-redlich-kwong and peng-robinson equations of state. Emirates Journal for Engineering Research, 2008. **13**(3): p. 81-91.

[39] Wei, Y.S. and R.J. Sadus, Equations of state for the calculation of fluid-phase equilibria. AIChE journal, 2000. **46**(1): p. 169-196.

[40] McCain Jr, W.D., Properties of petroleum fluids. 1973.

[41] Ahmed, T., Equations of state and PVT analysis. 2013: Elsevier.

[42] Vilagines, R.D. and A.R. Akhras. Three-phase flows simulation for improving design of gravity separation vessels. in SPE Annual Technical Conference and Exhibition? 2010. SPE.

[43] Kim, I.H., et al., Simulation-based optimization of multistage separation process in offshore oil and gas production facilities. Industrial & Engineering Chemistry Research, 2014. **53**(21): p. 8810-8820.

[44] Cui, Y., et al., Investigation of Influence of High Pressure on the Design of Deep-Water Horizontal Separator and Droplet Evolution. Processes, 2024. **12**(12): p. 2619.

[45] Arnold, B.F. and P. Stahlecker, *Linear regression analysis using the relative squared error.* Linear algebra and its applications, 2002. **354**(1-3): p. 3-20.